

PAPER • OPEN ACCESS

Study on Reverse Bending Characteristics in Straightening Process Considering the stress superposition

To cite this article: Yuanming Fang *et al* 2019 *IOP Conf. Ser.: Earth Environ. Sci.* **252** 022116

View the [article online](#) for updates and enhancements.

Study on Reverse Bending Characteristics in Straightening Process Considering the stress superposition

Yuanming Fang^a, He Ling^{*} and Hong Lu^b

School of Mechanical and Electronic Engineering, Wuhan University of Technology, Wuhan 430070, China

^{*}Corresponding author e-mail: linghe@whut.edu.cn, ^aFYM9610@163.com,

^blandzh@whut.edu.cn

Abstract. Straightening process is a typical dynamic process of multi-step reverse bending load. In adjacent straightening load, stress and strain will be superimposed with residual stress generated by straightening deformation energy influencing stress distribution state and reverse bending characteristics, particularly in the discrete points against bending straightening loading process. In order to describe the stress superposition state in process of straightening accurately, time operator is introduced to identify the discretization of straightening process and dynamic model characterized by curvature is created. Based on elastic-plastic mechanics and geometry hypothesis, the mathematical modeling of stress superposition state is established, and the relationship of discrete points reverse bending and straightening parameter in history is revealed.

1. Introduction

Straightening theory based on the mechanism of elastic-plastic deformation of workpiece during straightening process is the basic principle of various straightening schemes [1, 2, 3]. The main study object is workpiece deformation before and after the straightening process. In common straightening process, the principle of metal elastoplastic deformation is used, loading workpiece produces plastic deformation and the deformation direction is opposite to workpiece straightness error, until plastic deformation is equal to straightness error, or straightness error meets design requirements [4, 5, 6]. In the straightening process of some metal rods with special precision requirements, such as guide rail of machine tool, reverse bending method with good precision controllability is often used during finish-machining of straightening. Reverse bending is an effective method to improve straightness accuracy of workpiece, and its machining process is a nonlinear elastic-plastic deformation process [7, 8, 9,10]. Due to the existence of reverse bending residual deformation in discrete loading method, stress distribution of workpiece has some coupling relationship with its bending behavior. This feature influences subsequent bending behavior of workpiece and selection of bending parameters. Therefore, stress superposition characteristics is not negligible in high accuracy straightening process.



2. The residual stress model of straightening process

2.1. Residual stress distribution state

The workpiece per unit length is analyzed in process of straightening. As shown in Fig.1, C_0 is initial curvature of straightening. The cross-section a_0b_0 and neutral layer of workpiece intersect at the point of e_1 . After the reverse bending, the biggest reverse bend curvature is C_b , and cross section shape is unchanged. The section of a_0b_0 becomes a_1b_1 . The section of a_1b_1 becomes a_2b_2 after elastic recovery. The length of arc $\widehat{oe_0}$ and $\widehat{oe_1}$ and $\widehat{oe_2}$ all are equal to 1. Separately drawing corresponding arc length of a_0 and a_1 points to the cross section where elastic recovery happened, then the point of a'_0 and a'_1 are gotten, similarly the point of b'_0 and b'_1 are gotten. Therefore, on the surface of workpiece, the relationship of strain in geometric modeling can be shown as follow: total strain: $\varepsilon_\Sigma = \widehat{a'_0a'_1}$, residual strain: $\varepsilon_r = \widehat{a_2a'_1}$, elastic recovery strain: $\varepsilon_{sp} = \widehat{a'_0a_2}$.

The slash shadow area is residual stress. h_e is the thickness of elastic deformation area. σ_d and ε_d are maximum stress and strain of boundary layer. σ_s and ε_s are stress and strain of the yield limit. Under action of loading force F and based on flat section assumption. We can get $\varepsilon_{sp} = C_{sp}H/2$. Because elastic recovery is belong to pure elastic bending. We can get $C_{sp} = M_{sp}/EI = \bar{M}\bar{\sigma}_s/EI$, and $\varepsilon_{sp} = C_{sp}H/2 = \bar{M}\bar{\sigma}_sH/2EI = \bar{M}\bar{\sigma}_s/E$. The total strain: $\varepsilon_\Sigma = \varepsilon_{sp} + \varepsilon_r$, residual strain: $\varepsilon_r = \varepsilon_\Sigma - \varepsilon_{sp} = \sigma_s/E - \bar{M}\bar{\sigma}_s/E = \sigma_s(1 - \bar{M})/E$. Residual stresses on the surface: $\sigma_r = E\varepsilon_r = \sigma_s(1 - \bar{M})$.

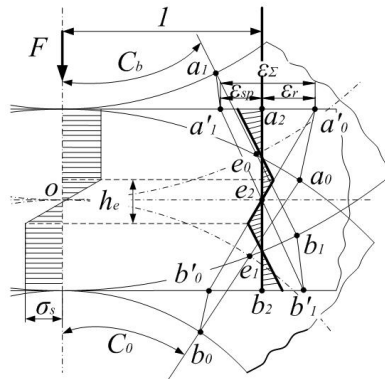


Fig. 1 Stress distribution state before and after straightening

2.2. Coupling mechanism between straightening process and stress evolution

Three-point reverse bending straightening adopts segmented and discrete loading point straightening method, which has characteristics of discretization [11,12]. Based on reverse bending dynamic model of straightening process, temporal factor is introduced to describe stress evolution. The number of straightening times is set to i , and upper mark (t_i) is used to describe straightening sequence. At this time, reverse bending straightening stress distribution of cross-section is $\sigma_\Sigma^{(t_i)}$. When $i = 1$, reverse bending stress distribution can be expressed as:

$$\sigma_\Sigma^{(t_1)} = \sigma_b^{(t_1)} = \begin{cases} \sigma_s & \frac{\xi^{(t_1)}H}{2} \leq z \leq \frac{H}{2} \\ \frac{2zC^{(t_1)}\sigma_s}{H} & -\frac{\xi^{(t_1)}H}{2} \leq z \leq \frac{\xi^{(t_1)}H}{2} \\ -\sigma_s & -\frac{H}{2} \leq z \leq -\frac{\xi^{(t_1)}H}{2} \end{cases} \quad (1)$$

Residual stress $\sigma_c^{(t_1)}$ can be given as:

$$\sigma_c^{(t_1)} = \begin{cases} \sigma_s \left(1 - \frac{2z\bar{M}^{(t_1)}}{H}\right) & \frac{\xi^{(t_1)}H}{2} \leq z \leq \frac{H}{2} \\ \frac{2z\sigma_s}{H} (C^{(t_1)} - \bar{M}^{(t_1)}) & -\frac{\xi^{(t_1)}H}{2} \leq z \leq \frac{\xi^{(t_1)}H}{2} \\ -\sigma_s \left(1 + \frac{2z\bar{M}^{(t_1)}}{H}\right) & -\frac{H}{2} \leq z \leq -\frac{\xi^{(t_1)}H}{2} \end{cases} \quad (2)$$

The distribution of reverse bending stress with certain straightening history is the linear superposition of residual stress generated by previous straightening and current reverse bending stress.

$$\sigma_\Sigma^{(t_2)} = \sigma_b^{(t_2)} + \sigma_c^{(t_1)} \quad (3)$$

The critical point of elastic-plastic deformation of straightened section satisfies relation below:

$$\sigma_s = \sigma_b^{(t_2)} + \sigma_c^{(t_1)} \quad (4)$$

When elastic zone ratio $\xi^{(t_1)} = 1$, it shows that entire workpiece is in an elastic deformation state, straightening process is finished. According to equation (2), it can be obtained that $\sigma = f(\xi^{(t_1)})$, σ is a function of $\xi^{(t_1)}$. Due to elastic zone ratio $\xi^{(t_1)}$ and $\xi^{(t_{i+1})}$ are different, classified discussion is necessary.

The direction of second straightening may be same as the first straightening or opposite. When direction is same, obviously $\xi^{(t_2)} < \xi^{(t_1)}$, all straightening residual stress effects of first time will disappear. When direction is opposite, the magnitude of two elastic zone ratio is uncertain. When $\xi^{(t_2)} < \xi^{(t_1)}$, all straightening residual stress effects of first time will disappear the same. So the problem can be divided into three categories.

(i) When $\xi^{(t_2)} > \xi^{(t_1)}$, the ideal straightening condition, posterior straightening elastic deformation area is larger than previous one, elastic zone ratio $\xi^{(t_1)}$ will approach to 1 as straightening processing. At this time, second straightening direction is opposite of first straightening. According to equations (2), (3) and (4), the distribution of the second loading stress can be given as:

$$\sigma_\Sigma^{(t_2)} = \begin{cases} -\sigma_s & \frac{\xi^{(t_2)}H}{2} \leq z \leq \frac{H}{2} \\ \frac{2zC^{(t_2)}\sigma_s}{H} + \sigma_s \left(1 - \frac{2z\bar{M}^{(t_1)}}{H}\right) & \frac{\xi^{(t_1)}H}{2} \leq z \leq \frac{\xi^{(t_2)}H}{2} \\ \frac{2zC^{(t_2)}\sigma_s}{H} + \frac{2z\sigma_s}{H} (C^{(t_1)} - \bar{M}^{(t_1)}) & -\frac{\xi^{(t_1)}H}{2} \leq z \leq \frac{\xi^{(t_1)}H}{2} \\ \frac{2zC^{(t_2)}\sigma_s}{H} - \sigma_s \left(1 + \frac{2z\bar{M}^{(t_1)}}{H}\right) & -\frac{\xi^{(t_2)}H}{2} \leq z \leq -\frac{\xi^{(t_1)}H}{2} \\ \sigma_s & -\frac{H}{2} \leq z \leq -\frac{\xi^{(t_2)}H}{2} \end{cases} \quad (5)$$

The following results can be gotten by integrating stress distribution state:

$$M^{(t_2)} = \int_{-H/2}^{H/2} \sigma_\Sigma^{(t_2)} z dz = \frac{3}{2} - \frac{1}{2C^{(t_1)}} + \left(-C^{(t_2)} + \frac{1}{2(C^{(t_1)})^2} - \frac{3}{2}\right)(\xi^{(t_2)})^3 \quad (6)$$

In formula (6), $C^{(t_1)} > 0$ and $C^{(t_2)} < 0$. In rare cases, posterior straightening elastic deformation area is smaller than previous one. When $\xi^{(t_{i+1})} < \xi^{(t_i)}$, elastic zone significantly reduced, and plastic zone increases, stress outside of elastic deformation zone $h_e^{(t_{i+1})}$ is σ_s , stress inside of elastic deformation zone is the superposition of residual stress and straightening stress.

(ii) When $\xi^{(t_2)} < \xi^{(t_1)}$, the second straightening direction is same as the first time, the stress

distribution is given by:

$$\sigma_{\Sigma}^{(t_2)} = \begin{cases} \sigma_s & \frac{\xi^{(t_2)}H}{2} \leq z \leq \frac{H}{2} \\ \frac{2zC^{(t_2)}\sigma_s}{H} + \frac{2z\sigma_s}{H}(C^{(t_1)} - \bar{M}^{(t_1)}) & -\frac{\xi^{(t_2)}H}{2} \leq z \leq \frac{\xi^{(t_2)}H}{2} \\ -\sigma_s & -\frac{H}{2} \leq z \leq -\frac{\xi^{(t_2)}H}{2} \end{cases} \quad (7)$$

The following results can be gotten by integrating stress distribution state as formula (6):

$$\bar{M}^{(t_2)} = \frac{3}{2} - \frac{3}{2}(\xi^{(t_2)})^2 + (C^{(t_2)} + C^{(t_1)} + \frac{1}{2(C^{(t_1)})^2} - \frac{3}{2})(\xi^{(t_2)})^3 \quad (8)$$

In formula (8), $C^{(t_1)} > 0$ and $C^{(t_2)} > 0$.

(iii) When $\xi^{(t_2)} < \xi^{(t_1)}$, the second straightening direction is opposite of first straightening, the stress distribution can be expressed as:

$$\sigma_{\Sigma}^{(t_2)} = \begin{cases} -\sigma_s & \frac{\xi^{(t_2)}H}{2} \leq z \leq \frac{H}{2} \\ \frac{2zC^{(t_2)}\sigma_s}{H} + \frac{2z\sigma_s}{H}(C^{(t_1)} - \bar{M}^{(t_1)}) & -\frac{\xi^{(t_2)}H}{2} \leq z \leq \frac{\xi^{(t_2)}H}{2} \\ \sigma_s & -\frac{H}{2} \leq z \leq -\frac{\xi^{(t_2)}H}{2} \end{cases} \quad (9)$$

The following results can be gotten by integrating stress distribution state as formula (6):

$$\bar{M}^{(t_2)} = -\frac{3}{2} + \frac{3}{2}(\xi^{(t_2)})^2 + (C^{(t_2)} + C^{(t_1)} + \frac{1}{2(C^{(t_1)})^2} - \frac{3}{2})(\xi^{(t_2)})^3 \quad (10)$$

In formula (13), $C^{(t_1)} > 0$ and $C^{(t_2)} < 0$. In cases of (ii) and (iii), expressions of $\bar{M}^{(t_2)}$ can be unified and can be considered same situation.

2.3. Multiple straightening iteration process and displacement prediction model.

According to classification discussed above, when $\xi^{(t_{i+1})} < \xi^{(t_i)}$, residual stress before can be eliminated at the $i + 1$ times, so in actual straightening process when $\xi^{(t_{i+1})} < \xi^{(t_i)}$, this straightening process can be regarded as last time straightening process. So multiple straightening processes stress distribution recursion can only be studied in the first case above.

The recurrence relations are as follows:

$$\sigma_{\Sigma}^{(t_{i+1})} = \begin{cases} (-1)^i \sigma_s & \frac{\xi^{(t_{i+1})}H}{2} \leq z \leq \frac{H}{2} \\ \frac{2zC^{(t_{i+1})}\sigma_s}{H} + \sigma_c^{(t_i)} & \frac{\xi^{(t_i)}H}{2} \leq z \leq \frac{\xi^{(t_{i+1})}H}{2} \\ \dots & \dots \\ \frac{2zC^{(t_{i+1})}\sigma_s}{H} + \sigma_c^{(t_i)} & -\frac{\xi^{(t_i)}H}{2} \leq z \leq -\frac{\xi^{(t_i)}H}{2} \\ \dots & \dots \\ \frac{2zC^{(t_{i+1})}\sigma_s}{H} & -\frac{\xi^{(t_{i+1})}H}{2} \leq z \leq -\frac{\xi^{(t_i)}H}{2} \\ (-1)^{i+1} \sigma_s & -\frac{H}{2} \leq z \leq -\frac{\xi^{(t_{i+1})}H}{2} \end{cases} \quad (11)$$

And $\xi^{(t_{i+1})}$ can be obtained by setting $z = \xi^{(t_{i+1})}H/2$ in the formula (11).

Then establish mathematical model of deflection and load in the three-point reverse bending process. The length of material is $2L$, intermediate loading force is F , and elastic plastic bending area is $2L_e$. Bending moment at coordinates x is M_x , so $M_x = (L - x)F/2$. Straightening deflection in the middle is:

$$\delta_{\Sigma} = \int_0^L dy = \int_0^L (L - x) A_x dx \quad (12)$$

In elastic region, A_x is a linear function, at this time. $A_x = M_x/EI = (L - x)F/2EI$. In elastic-plastic deformation area A_x is nonlinear function, because \bar{M} is a function of ξ , and $A_x = A_e C_x = A_e/\xi$, then $A_x = f(\bar{M})$. Therefore, above formula can be expressed as:

$$\delta_{\Sigma} = \int_0^{L-L_e} (L - x) A_x dx + \int_{L-L_e}^L (L - x) A_x dx = \frac{FL_e^3}{6EI} + \int_0^{L-L_e} (L - x) A_x dx \quad (13)$$

And $\bar{M} = Fx/FL_e = x/L_e$. The load-deflection equation is established according to straightening theory as follows:

$$F = \begin{cases} \frac{6EI}{L^3} \delta & 0 < F < F_e \\ \delta_{\Sigma} = \frac{FL_e^3}{6EI} + \int_0^{L-L_e} (L - x) A_x dx \\ \quad \frac{x}{L_e} = \bar{M}(\xi), A_x = \frac{C_x M_e}{EI} & F_e < F < F_p \\ \frac{6EI}{L^3} (\delta - \delta_0) & 0 < F < F_p \end{cases} \quad (14)$$

3. Straightening experiment and simulation of linear guide

3.1. Theoretical calculation and finite element simulation

Material parameters which are same as follow experimental data are selected for theoretical calculation. Material is 45 square steel. Straightening spans are 200mm, 350mm and 500mm respectively, and the section length and width are both 20mm. According to prediction model of straightening stroke mentioned above, specific parameters of materials are substituted, and MATLAB is used to calculate straightening stroke of linear guide with different initial deflections.

Using ANSYS finite element analysis method (FEM), the linear guideway model with different initial deflections are established. Straightening stroke estimated according to theory is simulated in workbench, and simulation distribution diagrams of initial deflection-straightening stroke are obtained. Relationship diagrams of calculated initial deflection-straightening stroke are shown Fig. 3

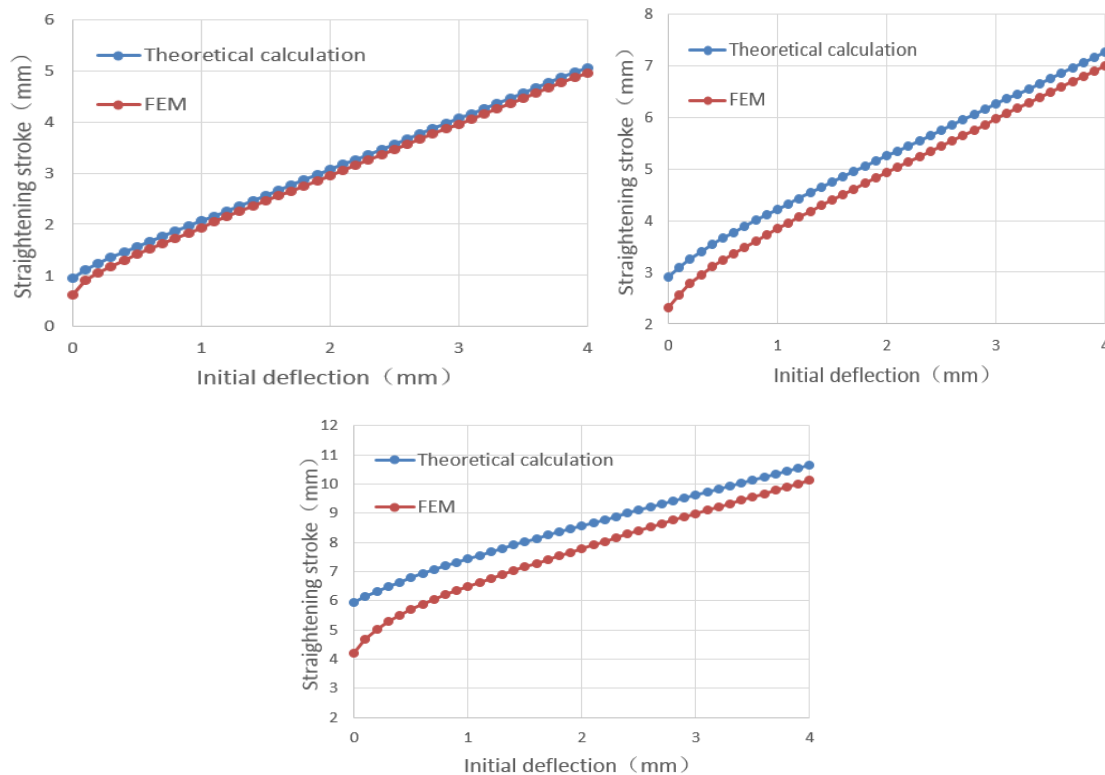


Fig. 2 200mm, 350mm, 500mm linear guide deflection - straightening stroke distribution

3.2. Experimental verification

3.2.1. Straightening experimental materials and procedures. In this straightening experiment, three-point reverse straightening method is adopted. The self-developed precision CNC straightening machine is used for online straightening experiment, and displacement sensor mounted on straightening machine is used to measure deflection value of loading point online. The experimental material are same as theoretical calculation.



Fig. 3 Numerical control straightening machine diagram and experimental

Specific experimental steps are as follows: (1) Selecting a number of linear guides of same size numbered 1-10. (2) Guide no.1 is straightened in same direction for 6 times. The absolute values of straightening coordinates are S1, S2, S3, S4, S5 and S6 respectively, and straightening stroke increases gradually. (3) Conducting 6 times of straightening for guide no.2, and direction of each straightening is different from previous one. The absolute values of straightening coordinates are S1, S2, S3, S4, S5

and S6. (4) Making 6 times of straightening for no.3 guide, and direction of each straightening is different from previous one. The absolute value of straightening coordinates are S6, S5, S4, S3, S2 and S1, straightening stroke gradually decreases. (5) Single straightening is performed for guide no.4-8. Absolute values of the straightening coordinates are S2, S3, S4, S5 and S6. (6) Straightening linear guide no.9 by using single straightening stroke prediction model and no.10 by using straightening stroke prediction model which considers residual stress superposition. Recording initial deflection, straightening stroke and residual deflection data above.

3.2.2. Experimental results and analysis. (1) First diagram is about multiple straightening in same direction and different direction straightening with $\xi(t_2) < \xi(t_1)$ versus single straightening. (2) Second diagram is about multiple different direction straightening and $\xi(t_2) > \xi(t_1)$ compares with single straightening. (3) Third diagram shows comparison between prediction model of multiple straightening considering stress superposition and prediction model of single straightening. (4) Last diagram is comparison of theoretical calculation, FEM and straightening experiment deflection-straightening stroke.

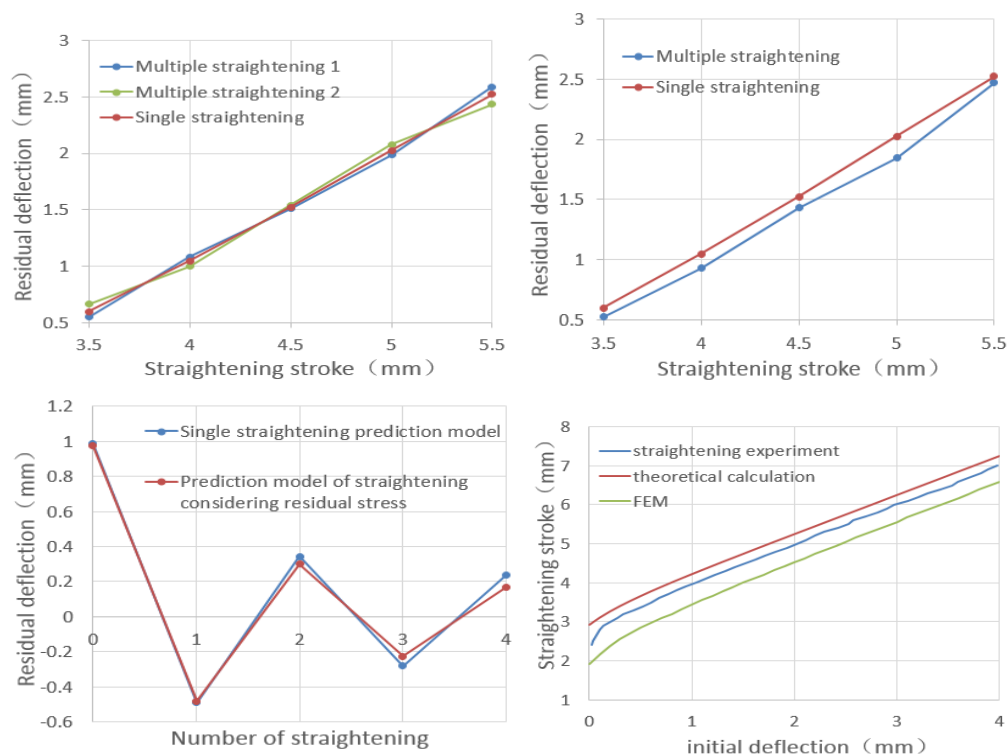


Fig. 4 Experimental results diagrams

Through comparison (1), it can be obtained that same direction multiple straightening and different direction multiple straightening with $\xi(t_2) < \xi(t_1)$ have no residual stress effect on latter one. Through (2), it can be obtained that former straightening of multiple different directions with $\xi(t_2) > \xi(t_1)$ has certain residual stress effect. Through (3), in process of multiple straightening, residual deflection value tends to converge, straightness error gradually decreases, which indicates correctness of the stroke prediction model, and convergence of repeated straightening is more accurate than single prediction model. Through (4), theoretical calculation and FEM straightening stroke prediction methods are correct and reliable within a certain error range.

4. Conclusion

The method of time series factor is used to describe straightening history and to distinguish the influence of different straightening processes on reverse bending characteristics. According to the mathematical description of discrete loading history reverse bending process, straightening parameters are correlated with straightening history and residual stress. In order to improve the accuracy of straightening, reverse bending parameters are required to be matched to obtain precise relationship of reverse bend curvature and reverse bending characteristic parameters. Elastic zone ratio change is related to straightening history, using prediction model of multiple straightening considering stress superposition, the control of straightening stroke will be improved.

Acknowledgments

This work was financially supported by “NSFC. No. 51505355 and No. 51675393”. We would like to thank NSFC for funding our project. We are very grateful to those who helped us to finish the work. Special thanks go to He Ling the corresponding author of the work.

References

- [1] Y.Q. Zhang, H. Lu, X.B. Zhang, W. Fan, H. Ling, Q.Y. Wei and M.T. Ma. A novel analytical model for straightening process of rectangle-section metal bars considering asymmetrical hardening features. *Advances in Mechanical Engineering*, 2018, 10 (9):1-14.
- [2] Yi Yali, Jin Herong. Three Roller Curvature Scotch Straightening Mechanism Study and System Design [J]. *Energy Procedia*, 2012, 16.
- [3] Y.Q. Zhang, H. Lu, H. Ling, Y. Lian and M.T. Ma. Analytical Model of a Multi-Step Straightening Process for Linear Guideways Considering Neutral Axis Deviation, Symmetry, 2018, 10 (8):316.
- [4] Jun Zhao, Xiaokang Song. Control strategy of multi-point bending one-off straightening process for LSAW pipes [J]. *The International Journal of Advanced Manufacturing Technology*, 2014, 72 (9-12).
- [5] Benjamin Leener MS, Gabriel Mangeat MS, Sara Dupont MS, Allan R. Martin MD, Virginie Callot PhD, Nikola Stikov PhD, Michael G. Fehlings MD, PhD, Julien Cohen-Adad PhD. Topologically preserving straightening of spinal cord MRI [J]. *Journal of Magnetic Resonance Imaging*, 2017, 46 (4).
- [6] Yoshida Kazunari, Sugiyama Tsuyoshi. 1424 Analysis of straightening of drawn wires using rollers by FEM [J]. *The proceedings of the JSME annual meeting*, 2008, 2008.1 (0).
- [7] Yong-Chen Pei, Jia-Wei Wang, Qing-Chang Tan, De-Zhi Yuan, Fan Zhang. An investigation on the bending straightening process of D-type cross section shaft [J]. *International Journal of Mechanical Sciences*, 2017, 131-132.
- [8] Kai Wang, Baoyu Wang, Chuancheng Yang. Research on the Multi-Step Straightening for the Elevator Guide Rail [J]. *Procedia Engineering*, 2011, 16.
- [9] Jialong Shen, Mujun Long, Dengfu Chen, Jian Zhang, Zhihua Dong. Analysis on the dynamic extension for transverse surface cracks in the as-cast steel slab at high temperatures [J]. *Engineering Failure Analysis*, 2016, 66.
- [10] Seung-Cheol Kim, Sung-Chong Chung. Synthesis of the multi-step straightness control system for shaft straightening processes [J]. *Mechatronics*, 2002, 12 (1).
- [11] Hong Lu, He Ling, Jae-Youn Jung, Xiao Zhang, Changqiao Guo. Bending properties of GCr15 steel guide rail under the multi-step loading [J]. *Journal of Wuhan University of Technology-Mater. Sci. Ed.*, 2010, 25 (4).
- [12] Jialong Shen, Mujun Long, Dengfu Chen, Jian Zhang, Zhihua Dong. Analysis on the dynamic extension for transverse surface cracks in the as-cast steel slab at high temperatures [J]. *Engineering Failure Analysis*, 2016, 66.